Modelling of Ejector Refrigeration System and Its Application to the Design of an Ejector Cooler for a Hot-Spring Resort in the Philippines

Menandro S. Berana and Glen D. Espeña

Abstract— **The heat-driven ejector refrigeration system offers the advantage of simplicity and can operate from low-temperature heat energy sources; thereby, it proves to be a good substitute to the conventional compressor-driven refrigeration system when any or a combination of heat sources is available. The Philippines is rich with renewable energy sources such as solar, geothermal energy, biomass and waste heat. Due to its location, it has a great deal of potential for geothermal resources. The low-enthalpy hot water spring has potential use in an ejector cooling system.**

In this paper, a mathematical model is developed for the ejector refrigeration system using one-dimensional flow and a friction model. The developed model is used in simulating the ejector cooling system for R134a, R152a and R1270, to determine the optimized performance, ejector geometries and refrigerant for the system. Properties of fluid during the flow at the components of the ejector were determined. R1270 performs best among the three refrigerants which was simulated at a maximum COP of 0.53.

The research also discusses designing an ejector refrigeration system using hot spring water. An ejector cooler with a cooling capacity of 1.5 kW is designed for boiler temperature range of 70 degrees C to 110 degrees C, condenser temperature of 25 degrees C to 45 degrees C, and evaporator temperature of 0 degrees C to 10 degrees C. In this setup, the major function of the hot spring water is to provide a warm pool, and the residual heat will be used for cooling using refrigerant R134a, as a commonly available and cheap refrigerant. The computed COP varies from 0.1 to 0.53. It was also determined that the payback period in using the ejector cooling in this setup is around 3 years.

When heat is freely available, an ejector refrigeration system is a viable alternative to conventional vapor compression cycle. It is shown that excess heat from naturally hot water in a hot spring resort can still be used for cooling using the ejector refrigeration system.

Index Terms— **ejector, refrigeration, waste heat, geothermal, modelling**

Manuscript received February 24, 2016; revised April 13, 2016. The dissemination of this research is sponsored by the Engineering Research and Development Program (ERDT) of the Department of Science and Technology (DOST) of the Republic of the Philippines. The program is being managed and implemented by the College of Engineering of University of the Philippines–Diliman.

M. S. Berana is with the Department of Mechanical Engineering, College of Engineering, University of the Philippines – Diliman, Quezon City, 1101 Philippines (phone: +63-906-214-1782, +63-2-981-8500 loc 3130; fax: +63-2-709-8786; e-mail: menandro.berana@coe.upd.edu.ph).

G. D. Espeña is with the Department of Science and Technology, 3F DOST Central Office, General Santos Avenue, Taguig City, 1631 Philippines (e-mail: glen.espena@gmail.com).

I. Introduction

The Philippines is endowed with abundant sources of renewable energy such as solar, geothermal energy, biomass and waste heat. Due to its geographical location, it has a vast potential for geothermal resources, making it the second largest producer of geothermal energy in the world, next to the United States [1]. Table I shows the installed geothermal plant capacity of different countries around the world in 2013 [2].

Geothermal energy is more popularly associated with electricity generation, but it also has nonelectrical and direct-use applications. The harnessing of hot natural water from the foot of Mt. Makiling, located in the province of Laguna, Philippines, is one such direct-use application. Its use for recreational and therapeutic purposes has been developed long before geothermal plants were established in the country. Based on the Department of Energy data, there exist around 500 hot spring resorts in Laguna Province [3].

The heat-driven ejector refrigeration cycle, refer to Fig. 1, is similar to the conventional vapor compression cycle, except that the compressor is replaced by liquid feed pump, vapor generator and ejector. Increasing energy demand and energy cost, and at the same time greater awareness on the negative environmental impacts of the compressor-driven refrigeration system have contributed to the need to work on and improve alternative refrigeration technologies such as the ejector refrigeration system driven by heat which can be coming from renewable energy sources [4].

When a low-temperature heat source is available, the ejector refrigeration system is a good substitute to the vapor compression refrigeration system because the heat energy input is usually free. By adopting the proposed system, the cost of cooling operations significantly decreases compared to when the vapor compression system is used.

II. EJECTOR MODELLING

In order to maximize the resources, proper ejector design and analysis is required. The ejector, being the critical component of the system, determines the overall performance and efficiency of the refrigeration system. This study focuses on the optimization of the ejector design for actual operating conditions with the assumption that the other components of the refrigeration such as heat exchangers, pump and expansion device are already optimized within a certain range of applicable conditions. Adiabatic irreversible flow model is used for the ejector analysis, wherein entropy generation and frictional losses through the ejector are considered.

TABLE I
WORLD INSTALLED GEOTHERMAL PLANT CAPACITY

Country	Capacity (MW)
USA	3389
Philippines	1884
Indonesia	1333
Mexico	980
Italy	901
New Zealand	895
Iceland	664
Japan	537

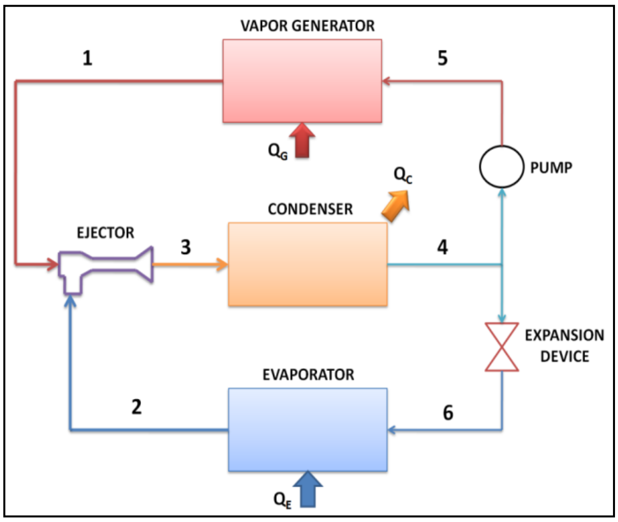

Fig. 1. Heat-driven ejector refrigeration system

The overall COP of the ejector system is expressed by eq. 1 or eq. 2. This involves the heat absorbed in the evaporator, the work of the pump and the heat energy input in the vapor generator. It can also be described in terms of mass flow rate of the primary and secondary fluids and their respective enthalpy.

$$COP_{system} = \frac{Q_{evap}}{W_{pump}+Q_{boiler}} \tag{1}$$

$$COP_{system} = \frac{\dot{m}_s(h_2-h_5)}{\dot{m}_p(h_1-h_4)} \tag{2}$$

For the ejector design, the study focuses on the ejector nozzle, pre-mixing chamber, the mixing section and the diffuser. Flow properties and ejector geometry are derived using the thermodynamic equations, conservation equations and other assumptions established based on literature. For this study, the authors used the following refrigerants: R134a, R152a and R1270.-

A. *Primary Nozzle*

The refrigerant coming from the vapor generator enters the primary nozzle of the ejector at high pressure and temperature but with negligible velocity. The primary nozzle is basically a converging-diverging nozzle. Fig. 2 demonstrates the division of the primary nozzle into elementary control volumes from the inlet up to the exit. It is assumed that the inlet properties of the fluid, which is at state 1, are all known. In order to determine the properties at state 2 after an increment distance dL, the conservation equations and thermodynamic relations are applied. The aforementioned equations are applied successively for every given distance until the exit of the nozzle is reached. The properties are calculated iteratively using Maruo Editor [5] and the Refprop thermodynamic database of the NIST [6].

The properties of the refrigerant entering the nozzle are known (P_1, T_1, h_1, s_1, v_1, μ_1, U_1 and A_1).In order to get the values in state 2 (P_2, T_2, h_2, s_2, v_2, μ_2, U_2 and A_2), conservation equations for mass, energy and momentum were applied together.

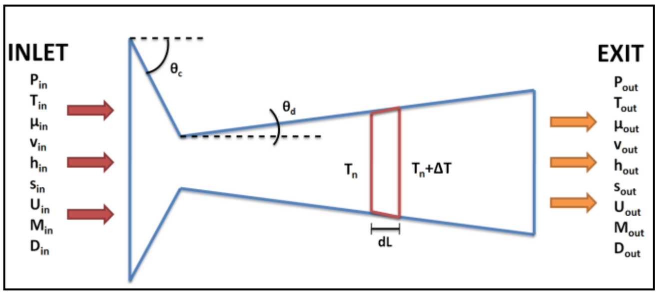

Fig. 2. Converging-diverging nozzle

For adiabatic process:

$$q_{cv} = 0 \tag{3}$$

Conservation of Mass:

$$\frac{U_1A_1}{v_1} = \frac{U_2A_2}{v_2} \tag{4}$$

Conservation of Energy:

$$-dh = d\left(\frac{U^2}{2}\right) \tag{5}$$

Conservation of Momentum:

$$-v\frac{dP}{dz} = \frac{d}{dz}\left(\frac{U^2}{2}\right) + 2f\frac{U^2}{D} \tag{6}$$

The Blasius-type friction factor was used in the analysis of ejector as expressed by the equation

$$f = CRe^{-n} \tag{7}$$

For the range of 3050 to 240,000 of Reynolds number, the value of *C* is 0.351 and n is equal to 0.225. But, for *Re* value of 240,000 and above, *C* is 0.118 and *n* is equal to 0.165, from the study of Joseph and Yang [7].

Velocity and area in the state 2 can be computed using eq. 8 and eq. 9, respectively.

ISBN: 978-988-14048-0-0
ISSN: 2078-0958 (Print); ISSN: 2078-0966 (Online)

$$U_2 = \sqrt{U_1{}^2 + 2(h_1 - h_2)} \tag{8}$$

$$A_2 = A_1 \frac{U_1}{U_2}\frac{v_2}{v_1} \tag{9}$$

The length of the controlled element for the converging and diverging section can be calculated using eq. 10 and eq. 11, respectively.

$$L = \frac{D_1\left(1-\sqrt{\left(\frac{U_1}{U_2}\right)\left(\frac{v_2}{v_1}\right)}\right)}{2tan\theta_c} \tag{10}$$

$$L = \frac{D_1\left(-1+\sqrt{\left(\frac{U_1}{U_2}\right)\left(\frac{v_2}{v_1}\right)}\right)}{2tan\theta_d} \tag{11}$$

The efficiency of the nozzle is the ratio of the actual change of kinetic energy to the isentropic change of the kinetic energy of the fluid from the inlet up to the nozzle exit, with the same pressure at the inlet state and pressure on the exit state. Therefore,

$$\eta_{nozzle} = \frac{\Delta KE_{nozzle,irr}}{\Delta KE_{nozzle,isen}} \tag{12}$$

B. *Pre-mixing Section*

The pre-mixing section is the portion comprised of the exit plane of the primary nozzle, the inlet plane of the secondary fluid and the inlet plane of the constant-area mixing section; see Fig. 3. The pre-mixing section was set apart from the mixing chamber to model and analyze separately the processes involved in each flow of the working fluid in order to determine the geometry of the ejector. In the pre-mixing section, there are no interactions or mixing of flow between the primary and the secondary fluids, making the analysis of each simpler and more accurate.

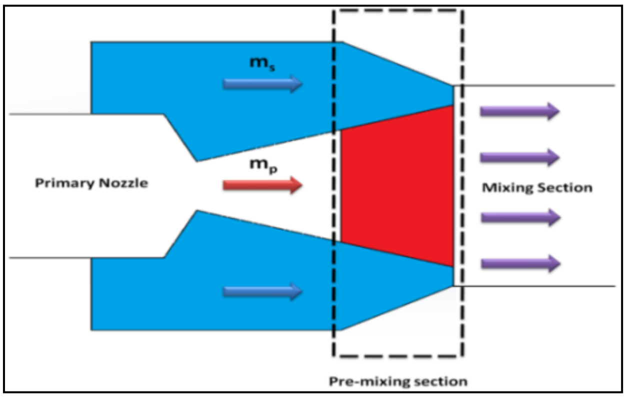

Fig. 3. The pre-mixing section

The primary fluid from the nozzle and the secondary fluid coming from the evaporator draw toward a plane in the inlet of the mixing section. The two fluids have different velocities, the primary being supersonic, while the secondary being subsonic, so there forms a sheer layer separating them. This “barrier” gradually becomes thinner until the fluids reach the inlet of the mixing chamber where they start to mix. It should be noted though that the mixing would only happen when the two fluids reach equal pressure and the Mach number of the secondary fluid is equal to unity, as assumed by Aphorrnratana and Eames [8]. The analysis of the controlled element in the primary and secondary flows is similar to the analysis used in the converging-diverging nozzle.

C. *Mixing Section*

The cylindrical-shaped component of the ejector with a constant-area is the mixing section. It is where the primary and secondary fluids start to interact, then fully mix and become a homogenous fluid flowing towards the inlet of the diffuser; refer to Fig. 4. Several thermodynamic processes arise during the mixing process. However, in this study, the main concern is to characterize the flow of the refrigerant before and after the mixing only.

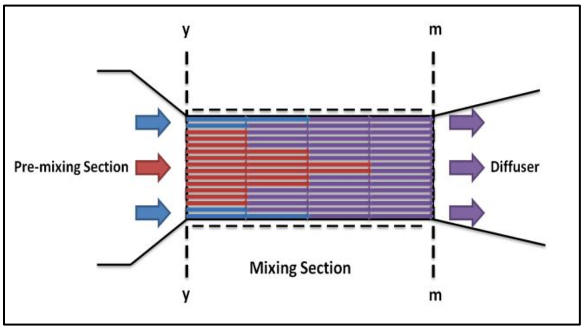

Fig. 4. The mixing section

The assumption of Sankarlal and Mani [9] on the diameter and pressure of mixing is also adopted in this paper. The diameter of the mixing section is assumed to be 10 times of the nozzle throat diameter to achieve the probability that the primary and the secondary flow mix at a constant pressure. In addition, the occurrence of the shock wave is contained within the assumed mixing length.

The velocity and quality of the fully mixed fluid in the mixing section is expressed by eq. 13 and eq. 14.

$$U_m = \frac{P_yA_{py}+U_{py}m_p+P_yA_{sy}+U_{sy}m_s+P_yA_{mix}}{m_p+m_s} \tag{13}$$

$$x_m = \frac{1}{h_{fg,m}}\left\{\begin{matrix} \left(\frac{m_p}{m_p+m_s}\right)\left[\left(h_{f,y} + x_{py}h_{fg,y}\right) + \frac{U_{py}^2}{2}\right] + \\ \left(\frac{m_s}{m_p+m_s}\right)\left[\left(h_{f,y} + x_{sy}h_{fg,y}\right) + \frac{U_{sy}^2}{2}\right] \\ -\frac{U_m^2}{2} - h_{f,m} \end{matrix}\right\} \tag{14}$$

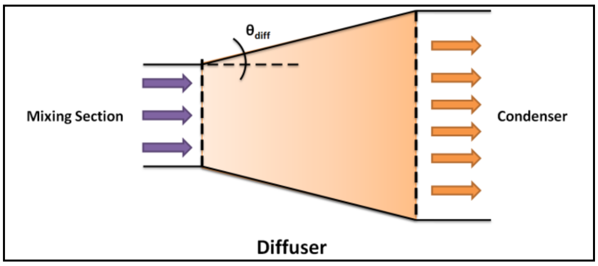

Fig. 5. The diffuser

D. *Diffuser*

The diffuser of the ejector is responsible for compressing the fluid to the condenser pressure, see Fig. 5. The available kinetic energy at the diffuser inlet is used to elevate the pressure. Thus, the flow velocity decreases as the fluid passes through the diffuser. The analysis of the controlled element in the diffuser is similar to the analysis used in the diverging nozzle.

III. CALCULATION RESULTS, DESIGN AND DISCUSSION

The main objective of this study is to come up with a design of an ejector for a particular operating condition that gives the maximum COP of the system. Aside from the geometry, all the required thermodynamic and flow properties across the ejector can be generated by the computer program using the Refprop thermodynamic database from NIST [6].

A. *Coefficient of Performance (COP)*

In eq. 1, the COP is defined as the ratio of the cooling capacity of the evaporator over that of the energy input in the vapor generator and feed pump. As shown in Fig. 6, as the vapor generator/boiler temperature increases, the coefficient of performance also increases. The maximum values are 0.095 for R134a, 0.0975 for R152a and 0.1075 for R1270. Maintaining the entrainment ratio and evaporator temperature, the condenser temperature increases as the vapor generator temperature increases. The decrease in enthalpy change in the vapor generator is larger compared to the decrease in the cooling capacity causing the COP to increase. R1270 has the highest COP compared to R134a and R152a within the range of vapor generator temperature of 70 °C to 110 °C. This can also be further explained in Fig. 7, where the COP decreases as the condenser temperature increases.

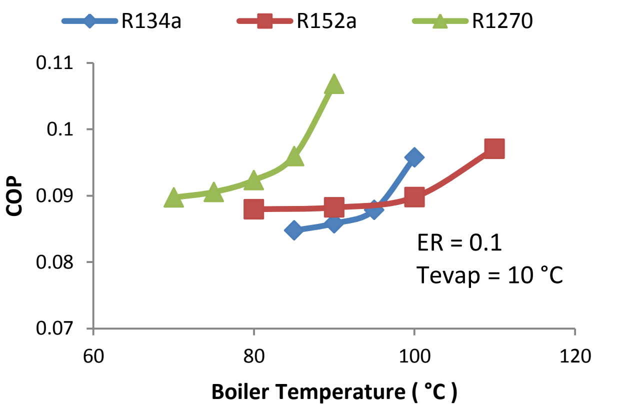

Fig. 6. Effect of vapor generator temperature to the COP

Fig. 7 shows the decrease in COP as the condenser temperature increases for the same vapor generator and evaporator temperature. The percentage increases are 80.283 % for R134a, 80.193 % for R152a and 79.857 % for R1270. This can be attributed to the decrease in the entrainment ratio as the condenser temperature is increased. For a constant mass flow rate in the evaporator, the increase in the primary mass flow rate is required to elevate the pressure of mixed fluid to higher condenser pressure. To be able to raise the mixed flow of refrigerant to a higher condenser pressure, an additional kinetic energy is necessary. With the increase in the primary mass flow rate, based on eq. 2, the COP decreases. For R 134 and R152a, the highest COP of 0.42 is obtained at a condenser temperature of 30°C while for R1270; the highest COP of 0.51 is achieved at almost 35 °C condenser temperature. A new model is introduced to maximize the geothermal energy, not only for heating the pool water in hot-spring resorts but also for cooling applications. Most of the hot-spring resorts have cooling requirements such as air conditioning and refrigeration systems for food and beverages. The proposed heat-driven ejector refrigeration system, as shown in Fig. 10, utilizes the heat of the hot geothermal water by reducing the temperature through the heat exchanger, converting it into cooling use and then pumping it into the swimming pool. With the ejector system, resort owners can benefit financially in using the renewable heat resource instead of electricity for cooling purposes.

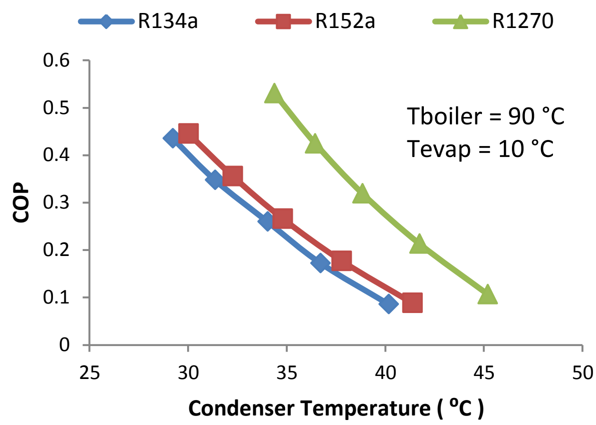

Fig. 7. Effect of condenser temperature to the COP

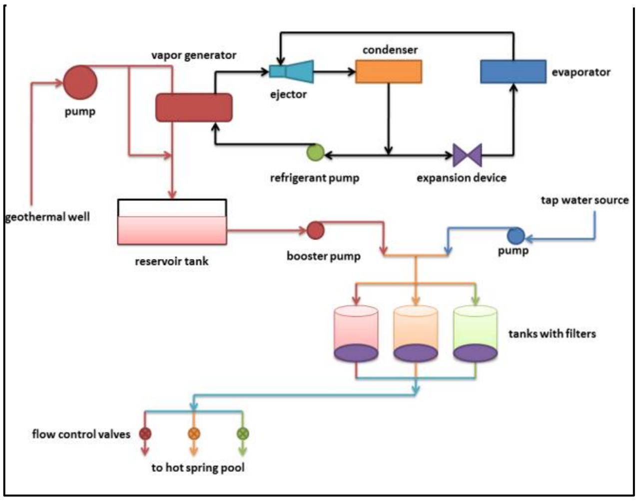

Fig. 8. Schematic diagram of the proposed ejector refrigeration system

B. *Design of Ejector Cooling System*

A new model is introduced to maximize the geothermal energy, not only for heating the pool water in hot-spring resorts but also for cooling applications. Most of the hot-spring resorts have cooling requirements such as air conditioning and refrigeration systems for food and beverages. The proposed heat-driven ejector refrigeration system, as shown in Fig. 8, utilizes the heat of the hot geothermal water by reducing the temperature through the heat exchanger, converting it into cooling use and then

ISBN: 978-988-14048-0-0
ISSN: 2078-0958 (Print); ISSN: 2078-0966 (Online)

pumping it into the swimming pool. With the ejector system, resort owners can benefit financially in using the renewable heat resource instead of electricity for cooling purposes.

For the actual application, the baseline-operating conditions as listed in Table II are set to determine the geometry of the ejector to be used in the proposed system

TABLE II
BASELINE CONDITIONS FOR EJECTOR DESIGN

Operating Conditions	Values
Refrigerant	R134a
Vapor Generator Temperature	90 °C
Condenser Temperature	40 °C
Evaporator Temperature	10 °C
Cooling Capacity	1.5 kW

The refrigerant that is chosen for this design is R134a because it is the most common and economical one among the non-ozone depleting refrigerant. Based on the operating conditions in Table II, a set of ejector geometry is derived from the mathematical model and is used in the proposed heat-driven ejector refrigeration system. The corresponding calculated ejector dimensions are shown in Table III.

TABLE III
EJECTOR DIMENSIONS

Specifications	
Nozzle Inlet Diameter	10.84 mm
Throat Diameter	2.96 mm
Nozzle Exit Diameter	5.00 mm
Suction Diameter	12.62 mm
Mixing Section Diameter	7.03 mm
Diffuser Outlet Diameter	13.33 mm
Primary Nozzle Length	9.59 mm
Throat Length	2.28 mm
Pre-mixing Section Length	2.67 mm
Mixing Length	70.36 mm
Diffuser Length	17.84 mm
Total Ejector Length	102.74 mm
Entrainment Ratio	0.1

The traditional vapor compression system utilizes electrical energy, largely by a compressor, to produce cooling, while the ejector system is powered by the geothermal energy and a pump to supply the cooling requirement. In comparing the two refrigeration systems, the main difference is on the economic aspect. The operation of the two systems is almost the same with the cooling capacity and operating time, so the cost of the equipment and the cost of operation is the deciding factor on which system has more economic benefits.

For the same expected operating conditions, the 1.5-kW cooling capacity, which is typical to a cooler, is used to evaluate the electrical consumption of the two systems. For the purpose of this paper, 0.27 USD is used as the average cost of electricity per kilowatt-hour in the Philippines.

The estimated average compressor consumption is about 750 W, while that of the ejector pump is 322 W running for 24 hours a day. These run times are considered in the comparison of the annual electric consumption of the two systems. Table IV shows the comparison of the equipment costs and the operational costs of the vapor compression cooler and the ejector cooler.

TABLE IV
COMPARISON IN EQUIPMENT AND OPERATIONAL COSTS

Cost (USD)	ERS	VCC
Equipment	2,227	795
Annual Electricity	762	1774

The required amount of energy to run the compressor in the vapor compression system is still much greater than the refrigerant pump of the ejector system. So even if the COP of the vapor compression system is higher compared to that of the ejector refrigeration system, the operational cost is less using the ejector system. The estimated payback period or breakeven point for using the ejector system versus the VCC is about 3 years which is considerably attractive. For the rest of service lives of the two systems, the ejector system offers the cheaper operating costs.

The paper expects to improve the operational efficiency of hot spring resorts, which can utilize geothermal energy using the ejector refrigeration system. The energy cost dedicated for cooling is lower with the use of the ejector refrigeration system, considering that the geothermal energy source is free. The owners only have to invest the equipment cost initially and retain the existing pumps used. The cost savings prove that the heat driven ejector system can be a substitute in providing cooling requirements of hot spring resorts.

IV. Conclusion

A mathematical model is developed for the ejector refrigeration system using one-dimensional flow incorporated with friction. The developed model is used in simulating the ejector cooling system for R134a, R152a and R1270, to determine the optimized performance, ejector geometries and refrigerant for the system. In the simulation, properties of fluid during the flow at the components of the ejector are determined. It is shown that R1270 performs best among the three refrigerants, simulated at a maximum COP of 0.53.

A heat-driven ejector refrigeration system is designed using the mathematical model to supply the cooling and refrigeration requirements of a hot spring establishment in the Philippines. The chosen location is abundant in geothermal energy in form of hot springs, wherein the hot water temperature is not enough for power generation but suitable for the ejector cooling system. An ejector cooler with a cooling capacity of 1.5 kW is designed for boiler temperature range of 70 degrees C to 110 degrees C, condenser temperature of 25 degrees C to 45 degrees C, and evaporator temperature of 0 degrees C to 10 degrees C. In this setup, the major function of the hot spring water is to provide a warm pool, and the residual heat will be used for cooling using refrigerant R134a as a commonly available safe refrigerant. The computed COP varies from 0.1 to 0.53. It was also determined that the payback period in using the ejector cooling in this setup is around 3 years, which is considerably attractive.

The cost savings prove that the heat-driven ejector refrigeration system is a feasible alternative to vapor compression system in providing the cooling requirements

ISBN: 978-988-14048-0-0
ISSN: 2078-0958 (Print); ISSN: 2078-0966 (Online)

of hot spring resorts. This study has established a novel way to effectively utilize hot spring water into useful and economical cooling through the ejector refrigeration system.

NOMENCLATURE

A	cross sectional area	(m^2)
C	Blasius friction-type factor coefficient	(-)
COP	coefficient of performance	(-)
D	hydraulic diameter	(m)
ER	entrainment ratio	(-)
f	homogeneous friction factor	(-)
h	enthalpy	(J/kg)
KE	kinetic energy	(m^2/s^2)
L	length	(m)
$\dot{m}$	mass flow rate	(kg/s)
n	Blasius index	(-)
P	pressure	(Pa)
Q	heat	(W)
RE	Reynolds number	(-)
s	entropy	(J/kgK)
U	velocity	(m/s)
v	specific volume	(m^3/kg)
x	quality	(-)
z	flow axis	(m)

Greek

θ	angle	(°)
η	efficiency	(-)

Subscripts

1	inlet, state point
2	outlet, state point
boiler	state in the boiler
c	converging
cv	control volume
d	diverging
diff	state in the diffuser
irr	irreversible
isen	isentropic
m	average/mean value
mixing	state in the mixing section
nozzle	state in the nozzle
p	primary flow
pump	state in the pump
py	primary flow at the inlet of mixing chamber
s	secondary flow; constant entropy
se	secondary fluid expansion
sy	secondary flow at the inlet of mixing chamber
y	mixing section inlet

ACKNOWLEDGMENT

The authors are sincerely thankful to the Engineering Research and Development for Technology (ERDT) Program of the Department of Science and Technology – Science Education Institute (DOST – SEI) of the Republic of the Philippines for funding this research and its dissemination.

REFERENCES

[1] Department of Energy [PH]. (2014). Geothermal. Retrieved from http://www.doe.gov.ph/renewable-energy-res/geothermal.
[2] B. Matek. 2013 Geothermal Power: International Market Overview, September 2013. Geothermal Energy Association
[3] A. F. Ulgado, M. T. M. Gular, (2005). Status of direct use of geothermal energy in the Philippines. The World Geothermal Congress 2005. Antalya, Turkey.
[4] K. Chunnanond,, S. Aphornratana, (2004). Ejectors: applications in refrigeration technology. Renewable and Sustainable Energy Reviews 8, 129–155.
[5] K. Saitou, (2007). Maruo Editor Version 7.07.
[6] E. W. Lemmon, M. O. McLinden, M. L. Huber, NIST Reference Fluid Thermodynamic and Transport Properties (REFPROP), Standard Reference Database 23, Version 8.0. National Institute of Standards and Technology (NIST), Gaithersburg, Maryland, 2007.
[7] D.D. Joseph, B.H. Yang, (2010). Friction factor correlations for laminar, transition and turbulent flow in smooth pipes. Physica D: Nonlinear Phenomena, Vol. 239, 1318-1328.
[8] S.Aphorrnratana, I.W. Eames (1997). A small capacity steam-ejector refrigerator: experimental investigation of a system using ejector with movable primary nozzle. International Journal of Refrigeration, Vol. 20, 352-358.
[9] T. Sankarlal, A. Mani (2007). Experimental investigations on ejector refrigeration system with ammonia. Renewable Energy, Vol. 32, 1403-1413.